International Journal of Chemistry; Vol. 9, No. 4; 2017
ISSN 1916-9698 E-ISSN 1916-9701
Published by Canadian Center of Science and Education

Effect of a 50-Hz Magnetic Field on the Degradation of Plasmid in the Presence of Cu(II) Ions and Hydrogen Peroxide

Yuuichi Kawashima[1], Honoka Fujii[1], Maresuke Nakayama[1], Masahiko Hasegawa[1], Satoru Shimanuki[1], Hidetake Miyata[1]

[1]Department of Physics, Tohoku University, Aramaki 6-3, Aoba-ku, Sendai, Miyagi 980-8578, Japan

Correspondence: Hidetake Miyata, Department of Physics, Tohoku University, Aramaki 6-3, Aoba-ku, Sendai, Miyagi 980-8578, Japan. E-mail: miyata@bio.phys.tohoku.ac.jp

Received: September 3, 2017 Accepted: September 24, 2017 Online Published: September 29, 2017

doi:10.5539/ijc.v9n4p40 URL: https://doi.org/10.5539/ijc.v9n4p40

Abstract

Power-line frequency (50/60 Hz) magnetic fields enhance DNA strand breaks in the cell. In order to understand the molecular mechanism underlying this phenomenon, we analyzed the conversion of plasmid from the supercoiled to the linear form. This conversion is promoted by hydroxyl radical generated by the reaction between Cu^{2+} and H_2O_2. The plasmid pHSG298 was incubated with 1 μM Cu^{2+} and 1 mM H_2O_2 and exposed to a 1.2 mT, 50-Hz magnetic field for 30, 60, and 90 min. The conversion of supercoiled DNA to linear DNA was analyzed by agarose gel electrophoresis. We found that exposure to the magnetic field for 90 min significantly enhanced the degree of conversion.

Keywords: extremely low frequency magnetic field, DNA strand breaks, supercoiled DNA

1. Introduction

There have been conflicting reports regarding the effect of power line magnetic fields on DNA. For example, Adair (2000) pointed out that the energy of a power-line frequency (in most cases 50/60 Hz) magnetic field is too low to cause strand breaks in cellular DNA, whereas a number of other studies demonstrated that double- or single-strand breaks (DSB/SSB) in cellular DNA are enhanced by 50/60 Hz magnetic fields (Zmyslony et al., 2000; Lai and Singh, 2004; Focke et al., 2010; Nakayama et al., 2014, 2016). It has been suggested that DNA strand breaks are due to cellular oxidative stress caused by the magnetic field (Mattsson and Simkó, 2012). This view is supported by observations that radical scavengers such as vitamin E (Kastir and Parola, 1998), melatonin (Jaite et al., 2001) and Trolox C (Lai and Singh, 2004) reduce the DNA breaking effect of magnetic fields.

Magnetic fields have been shown to enhance strand breaks in purified DNA exposed to oxidative stresses. For example, when the plasmid pGEM in the presence of H_2O_2 was exposed to a 250 mT static magnetic field, the original supercoiled form of the plasmid was converted to the open circular form, whereas this conversion was slower in the absence of the magnetic field (Potenza et al., 2004). Furthermore, the reaction between Cu^{2+} and H_2O_2 promotes conversion of supercoiled DNA to the linear form, and H_2O_2, Cu^{+}, Cu^{2+} and OH radical may participate in this reaction (Sagripanti and Kraemer, 1989). Li and Chow (2001) have shown that a 50-Hz magnetic field accelerates this conversion in the presence of Cu^{2+} + H_2O_2. Thus, a magnetic field likely enhances this conversion reaction under oxidative conditions.

How a 50/60 Hz magnetic field enhances the conversion of higher order DNA structures to the linear form is extremely important for understanding the mechanism by which a magnetic field strand breaks in cellular DNA. To achieve this goal, detail of how the magnetic field would affect the conversion process should be elucidated, but studies to date (Li and Chow, 2001; Potenza et al., 2004) have been insufficient in this regard. Thus, here we conducted a detailed analysis of how a 50-Hz magnetic field promotes the chemical conversion/degradation of plasmid DNA by Cu^{2+} + H_2O_2.

2. Method

2.1 Materials

Plasmid (pHSG298), the restriction enzyme (BamH-1), and 10X Loading buffer were obtained from Takara Bio (Tokyo, Japan). pHSG298 has 2675 base pairs and a single restriction site for BamH-1 (Takeshita et al., 1987). The plasmid was amplified in *Escherichia coli* strain DH5α and purified using a purification kit (NucleoBond®Xtra Midi, Machery-Nagel GmbH & Co. KG, Düren, Germany). Supercoiled DNA ladder marker and linear DNA ladder marker were obtained from New England BioLabs Inc. (Ipswich, MA) and Bayou Biolabs (Metairie, LA), respectively.

2-Amino-2-(hydroxymethyl)-1,3-propanediol (tris), $CuSO_4 \cdot 5H_2O$, acetic acid, and H_2O_2 were obtained from Wako Pure Chemical Industries (Osaka, Japan) and were of analytical grade. 2-[4-(2-Hydroxyethyl)-1-piperazinyl] ethanesulfonic acid (HEPES) and ethylene diamine tetraacetic acid (EDTA) were obtained from Dojindo Laboratories (Kumamoto, Japan). Water was first deionized and distilled with a water purification system (WG222S, Yamato Scientific, Tokyo, Japan) and further purified with a MilliQ system (Simplicity UV, Millipore, Tokyo, Japan). Agarose (Gene Pure LE) was obtained from BM Equipment Co., Ltd. (Tokyo, Japan). The DNA-staining agent Gel Red (10000X) was obtained from Biotium, Inc. (Hayward, CA).

2.2 Application of Magnetic Field

A 50-Hz sinusoidal magnetic field was applied to samples using a Helmholtz coil (U21901; 3B Scientific, Niigata, Japan). Each of the two coils was 130 mm in diameter and 100 turns of copper wire were wound around each coil. The center-to-center distance between the two coils was 65 mm. To generate the magnetic field, the current from a function generator (model WF1973, NF Corporation, Yokohama, Japan) was amplified with a power amplifier (model HSA4012, NF Corporation) and fed to the coil system. The current was adjusted to 0.8 A, and the flux density along the coil axis at the center of the two coils was 1.2 mT. The flux density of the magnetic field was measured at the coil center with a Hall-effect probe (Model MNT-4E04-VH or MMA-2502-VH, Lakeshore Cryotronix Inc., Westerville, OH) connected to a Gauss meter (Model 421, Lakeshore).

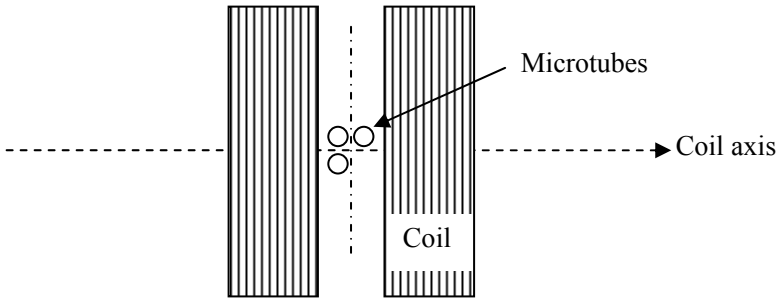

Figure 1. Top view of a pair of circular Helmholtz coils and the arrangement of 1.5 mL microtubes around the coil center

The diameter of mmicrotube was 1 cm; the center-to-center distance between the two microtubes was 1.25 cm. Microtubes containing samples were placed near the coil axis (dashed line) and the median plane (dot-dash line) of the two coils, where the spatial variation of the magnetic field was minimal.

2.3 Preparation of Plasmid Samples for Exposure

Three microtubes (AS ONE Corporation, Osaka, Japan) were placed near the center of the Helmholtz coil for exposure (exposure-coil; Figure 1: the center-to-center distance of the adjacent microtubes was 12.5 mm) and three additional tubes (control) were placed ~80 cm from the exposure-coil on the same table as the exposure coil. During exposure, the background magnetic field (20-2000 Hz) at the location of the non-exposed (control) samples was < 1 μT, as measured with a Gauss meter (Model 4190; FW Bell, Pacific Scientific-OECO, Milwaukie, OR). The room temperature was maintained with an air-conditioner at 24 °C and the day-to-day variability was < 0.5 °C. Temperatures were measured at each of the two sample locations using a K-type thermocouple connected to a digital voltmeter (model TR2114H, Advantest, Tokyo, Japan) and the difference between the two temperatures was at most 0.2 °C.

Prior to exposure, 10 μg/ml plasmid dissolved in buffer (40 mM tris, 2 mM EDTA, pH adjusted to 8.5 with acetic acid) was distributed to eight microtubes (10 μL for each tube). At appropriate times (depending on the experiment: e.g., 30 min) before the start of electrophoresis, 5 μL $CuSO_4$ (final concentration in the microtube was 1 μM, 10 μM or 100 μM, depending on the experiment) and 5 μL H_2O_2 (final concentration was 1 mM or 2.2 mM, depending on the experiment) were added to each microtube. Three of these microtubes were placed in the Helmholtz coil and another three samples were placed ~80 cm from the exposure coil, as described above. Following exposure/non-exposure for various lengths of time, the plasmid solution in each tube was subjected to electrophoresis in 0.8% agarose gel using a mini-gel electrophoresis apparatus (Mupid; Advance, Tokyo, Japan; field intensity = 9 V/cm). The 0 min samples were prepared as follows. The plasmid samples in the remaining two tubes were mixed with $CuSO_4$ + H_2O_2 plus the 10X Loading buffer and subjected to electrophoresis together with the exposed/non-exposed samples. Plasmid solution and the supercoiled ladder marker were mixed with 10X Loading buffer in two separate tubes and subjected to electrophoresis in the same gel.

2.4 Gel staining and Image Acquisition

Following electrophoresis, the gel was stained for 15 min at room temperature in electrophoresis buffer containing 1/10,000 volume of Gel Red solution. The stained gel was illuminated with a UV illuminator (TFP-35L, Vilber Lourmat, Cedex, France) and the DNA band pattern was acquired with a digital camera (5184 × 3456 pixels, 14 bit; Model 8574B, Canon, Tokyo, Japan). The exciation light coming from the area off the gel was blocked with aluminum foils placed around the gel; this significantly reduced the background light that interfered with the measurement of the intensity of DNA bands.

2.5 Analysis of the Gel Pattern

The fluorescence intensity of each band was quantitatively analyzed as follows. First, the fluorescence intensity of each lane was quantified with a plugin (Gel-analyzer) run on Image J. Second, the intensity profile of a lane with no sample (to correct distortion in the background arising from non-uniform illumination of the excitation light; seventh lane in Figure 4) was subtracted from the intensity profiles of the lanes containing DNA samples. Finally, the band intensities of supercoiled DNA part and linear DNA part were calculated and the resultant values were denoted I_{SC} and I_{LIN}, respectively.

A supercoiled DNA ladder marker or a linear DNA ladder marker was used as appropriate to estimate the number of base pairs comprising the DNA band. The $\log_{10}$ [base pair number] value of each marker band was plotted against the distance moved by the corresponding band to prepare a calibration curve.

3. Results

3.1 Confirmation of the Production of OH Radical

The degradation of DNA by Cu^{2+} ions and H_2O_2 depends on the presence of OH radical (Sagripanti & Kraemer, 1989). We confirmed this in two experiments. First, using a fluorescence spectrophotometer (FP-750, JASCO, Tokyo, Japan), we measured the increase in the fluorescence intensity at 425 nm upon excitation at 310 nm of 2.16 mM terephthalic acid in the presence of 0.54 mM Cu^{2+} + 1.08 mM H_2O_2 (Romanova et al., 1980; Barreto et al., 1995). The fluorescence intensity increased over a period of tens of minutes, indicating the continuous production of OH radical. Second, gel electrophoresis demonstrated that conversion of the plasmid from the supercoiled form to the linear form slowed in the presence of the radial scavengers 50 mM DMSO (Babbs and Gale, 1988) or 5 mM HEPES (Hicks and Gebicki, 1986).

3.2 Degradation of Plasmid in the Presence of 100 μM Cu^{2+} + 2.2 mM H_2O_2

We first adopted the chemical condition described by Li and Chow (2001). Figure 2 shows a typical result of the analysis by agarose gel electrophoresis: lane 1 shows the supercoiled ladder marker and lane 2 shows the untreated plasmid (supercoiled DNA; 2675 base pairs). Lanes 3 and 4 show plasmid treated with 100 μM Cu^{2+} + 2.2 mM H_2O_2 and not exposed (lane 3) or exposed (lane 4) to a 1.2 mT, 50-Hz magnetic field. After 15 min incubation and exposure, the plasmid band completely disappeared and there was no apparent effect of the magnetic field. Exposure for 15 min of plasmid DNA to up to a concentration of 1 mM Cu^{2+} ion alone or up to 2.2 mM H_2O_2 alone resulted in neither conversion nor degradation. Note that the presence of H_2O_2 alone resulted in a smear appearing above the supercoiled band, but the intensity was weak and no attempt was made to analyze this band.

3.3 Degradation of the Plasmid in the Presence of 10 μM Cu^{2+} + 1 mM H_2O_2

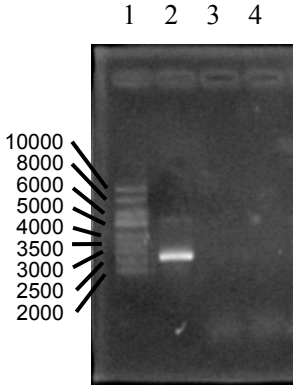

Figure 2. Plasmid exposed or not exposed to a 1.2 mT, 50-Hz sinusoidal magnetic field for 15 min in the presence of 100 μM Cu^{2+} and 2.2 mM H_2O_2. Lane 1, supercoiled DNA ladder marker; lane 2, untreated plasmid; lanes 3 and 4, plasmid treated with Cu^{2+} + H_2O_2 not exposed (lane 3) or exposed (lane 4) to the magnetic field

The plasmid band is evident in lane 2 (the untreated plasmid) but is absent in lanes 3 and 4, making quantification of the effect of the magnetic field impossible. Numbers on the left indicate the base pairs

We lowered the concentration of Cu^{2+} to 10 μM in order to observe the degradation process in more detail. As shown in Figure 3, after 15 min incubation of plasmid with Cu^{2+} + H_2O_2 under the non-exposure condition ("Non-exp, 15" in Figure 3, Panel (A)), all the supercoiled DNA had been degraded; a band with lower and higher mobilities appeared, as indicated with downward and upward arrowheads in the third lane. Similar fast degradation occurred for the exposed sample ("Exp, 15").

We found that the mobility of the band indicated with the downward arrowhead in the third lane was very similar to that of linear DNA obtained following the digestion of supercoiled DNA with BamH-1 (resulting in a single DSB at the sole restriction site (data not shown)): the number of base pairs comprising the former band as estimated from the semi-log plot was 2840 and that of the digested sample was 2880. Hence, we concluded that within experimental error, the major band with lower mobility corresponded to linear DNA generated by a single DSB of the supercoiled DNA. The minor band comprised 2670 base pairs and we presumed that it was generated by further degradation by the DSB of linear DNA. This band became fainter at later time points (the fourth, fifth and the sixth lanes). Concomitant with the disappearance of this band, the smear became more apparent (the asterisks in the fifth and sixth lanes). These changes suggest that OH radical converted the plasmid DNA from the supercoiled to the linear form by a single DSB, followed by additional degradation.

When plasmid was exposed to a 1.2 mT, 50-Hz magnetic field, the degradation pattern appeared similar to that of the non-exposed sample (Figure 3, Panel (A), the eighth to eleventh lanes). However, close inspection of the gel pattern suggested that the degradation of linear DNA was slightly faster in the exposed group, as indicated by the fainter smear at 40 and 60 min (Figure 3, Panel (A) asterisks in the fifth and sixth lanes and those in the tenth and eleventh lanes). This difference is represented semi-quantitatively in Figure 3, panel (B), in which the fluorescence intensities of the fifth lane (gray line) and the tenth lane (black line) are compared. The fluorescence intensity around the region indicated by the downward arrow was lower for the exposed sample than for the non-exposed sample. Similar gel patterns were observed in two out of four independent experiments; in the other two experiments, the plasmid band degraded within shorter time periods, and the effect of the magnetic field could not be assessed. The gel pattern showing an effect of the magnetic field is similar to that previously presented by Li and Chow (2001).

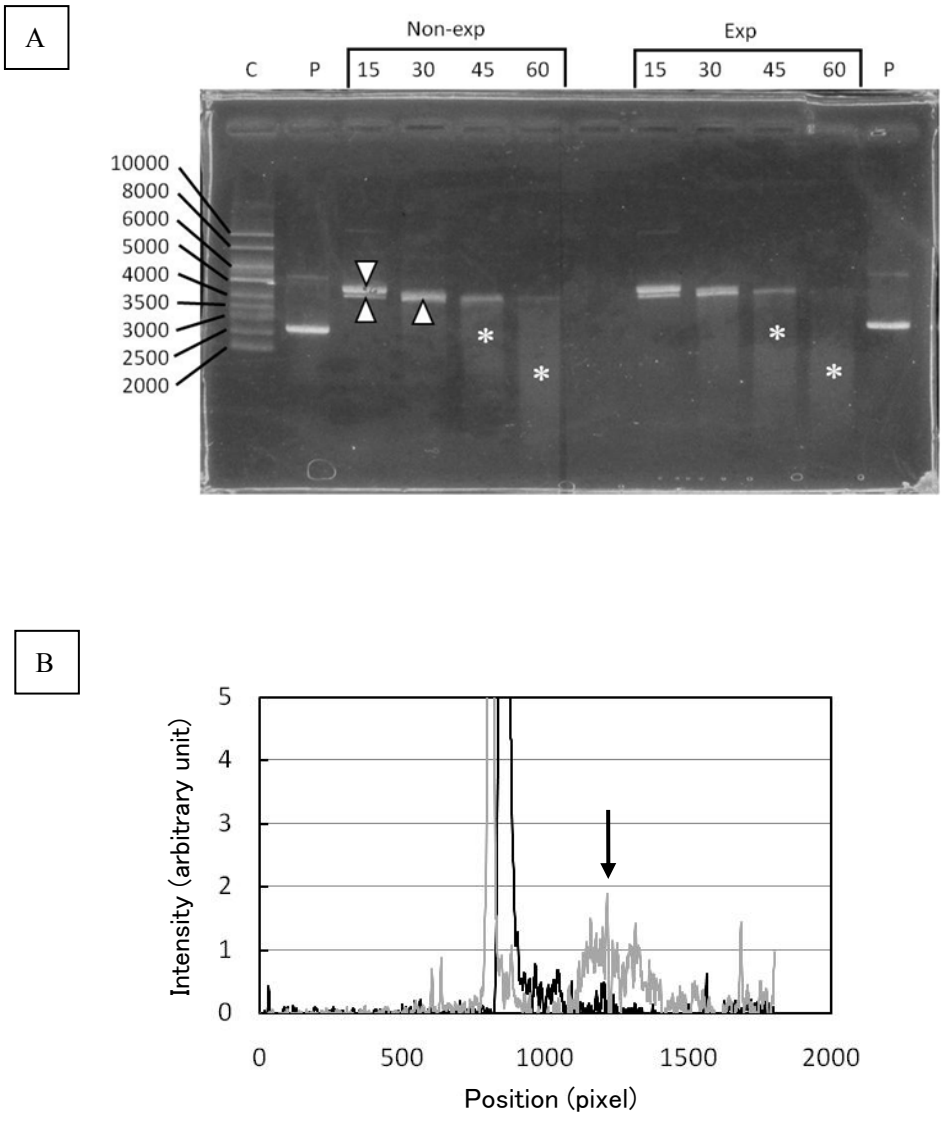

Figure 3. Degradation of DNA in the presence of 10 μM Cu^{2+} + 1 mM H_2O_2

Panel (A), "Non-exp" and "Exp" above the gel indicate non-exposure and exposure, respectively. The first lane (C) shows supercoiled ladder markers: numbers on the left indicate the number of base pairs. The second and the last lanes (P) contain untreated plasmid. The labels 15, 30, 45 and 60 above the gel denote the time in minutes after the start of non-exposure/exposure treatment. In the non-exposed sample, the major band (downward arrowhead) in the third lane is linear DNA generated by a single DSB; a minor band (upward arrowhead) immediately below was probably generated from the linear DNA by further DSB. This was the only band at 30 min (the upward arrowhead in the fourth lane). At later time points, this band became fainter and smears appeared (asterisks in the fifth and the sixth lanes). The exposed sample provided a similar gel pattern (see text for details). Panel (B), the fluorescence intensities of samples not exposed (gray line) or exposed (black line) to the magnetic field for 45 min. The fifth and tenth lanes in Panel (A) are compared. The downward arrow in the graph indicates the region showing the most prominent differences in the two intensity traces. The slight shift in the location of the major peak in the graph is due to distortion in the gel and not to different mobilities of the bands.

3.4 Degradation of plasmid in the presence of 1 μM Cu^{2+} + 1 mM H_2O_2

We further lowered the concentration of Cu^{2+} and observed that degradation of the plasmid also occurred (Figure 4,

second to sixth lanes and eighth to eleventh lanes; the seventh lane was used for background measurement). Importantly, during the timeframe of the experiment (from 30 min to 90 min), linear DNA (e.g., the downward white arrow in lane 5) coexisted with supercoiled DNA (upward white arrow in lane 5). At 30 min, roughly half the plasmid DNA was in the supercoiled form.

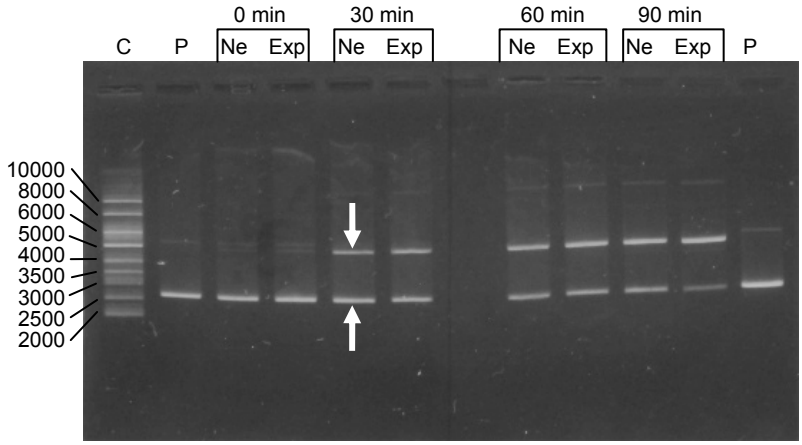

Figure 4. A typical agarose gel pattern used to analyze the degradation of supercoiled plasmid in the presence of 1 μM Cu^{2+} + 1 mM H_2O_2 with or without exposure to a magnetic field

The first lane (C) contains supercoiled ladder marker; the second and the twelfth lanes (P) contain untreated plasmid. The time periods for non-exposure/exposure to the magnetic field are indicated on the top (0 min, 30 min, 60 min and 90 min). Ne and Exp represent non-exposure and exposure, respectively. Non-exposed and exposed samples obtained at each time point are placed side-by-side to facilitate comparison of the effect of the magnetic field. At 30, 60 and 90 min, there were only two major bands: supercoiled DNA (e.g., upward white arrow in the fifth lane) and linear DNA (downward white arrow in the same lane). A minor band with lower mobility than that of the linear DNA band is seen (0 min) but was omitted from quantitative analysis due to its small amount.

The results of quantitative analysis of this conversion are shown as a plot of the ratio I_{LIN}/I_{SC} against the length of exposure (Figure 5, main graph). I_{LIN}/I_{SC} monotonically increased with time for both the non-exposed and exposed samples. However, at 60 min, the ratio of the exposed sample (closed diamond) was 1.14 times higher than that of the non-exposed sample (open diamond), and at 90 min it was 1.37 times higher (statistically significant: $P = 0.036$, paired *t*-test; ten independent experiments). Thus, we conclude that a 1.2-mT, 50-Hz magnetic field accelerated the chemical conversion of supercoiled DNA to linear DNA.

We evaluated the effect of a 50-Hz magnetic field on the DNA in the smear below the linear DNA band. The fluorescence intensity was measured in each lane at locations below the linear DNA and summed, then, the sum of the intensity of the supercoiled and linear DNA was subtracted. We assumed that the difference between the two sums was proportional to the amount of DNA in the smear. As shown in the inset of Figure 5, the smear remained essentially constant until 30 min after initiating exposure, then rapidly decreased, suggesting further degradation of the DNA in the smear. Up to 60 min, there was no difference between the non-exposed and exposed samples, but at 90 min, the fluorescence intensity of the smear was 1.6 times lower in the exposed sample than in the non-exposed sample ($P = 0.026$, paired *t*-test; ten independent experiments). This suggests that the degradation of DNA fragments in the smear generated by multiple DSBs was also accelerated by the magnetic field, and this occurred on the same time scale as the acceleration of the conversion from the supercoiled- to the linear-form.

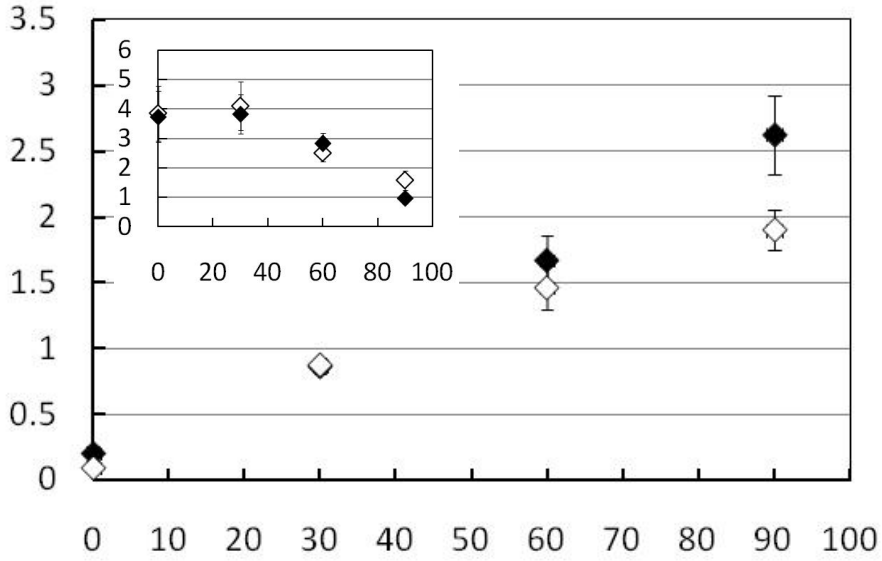

Figure 5. Quantification of the gel pattern shown in Figure 4

Main graph: the ratio I_{LIN}/I_{SC} is plotted against the length of non-exposure/exposure treatment (in min). The open and closed diamonds represent non-exposed and exposed samples, respectively. *Inset*: Ordinate, the fluorescence intensity (in arbitrary units) of the smear (see text for an explanation); abscissa, the duration of exposure in minutes. The data are the same as used to construct the main graph. In the main graph and the *inset*, bars represent the standard error (experiments under each condition were repeated ten times). *: $P = 0.036$ in the main graph; $P = 0.026$ in the inset at 90 min (both from two-tailed paired *t*-tests).

3.5 Effect of the Magnetic Field on DSB by Horseradish Peroxidase in the Presence of H_2O_2

The OH radical is also generated from the decomposition of H_2O_2 catalyzed by horse radish peroxidase (Chen and Schopfer, 1999). We investigated if a 50-Hz magnetic field affects this reaction. Degradation of the plasmid by horse radish peroxidase (10 μg/mL) + 1 mM H_2O_2 was observed, but a 1 mT, 50-Hz magnetic field had no effect on the degradation pattern of plasmid DNA.

3.6 Effect of the Magnetic Field on the Conversion of Plasmid by the Fe-Fenton Reaction

The Fe-Fenton reaction (generation of radical by Fe^{2+} + H_2O_2) also causes DNA strand breaks (Yamazaki and Piette, 1991; Luo et al., 1994; Henle and Linn, 1997). We investigated if a 50-Hz magnetic field would affect the strand breaks promoted by the Fe-Fenton reaction. We observed the degradation of plasmid DNA in the presence of 5 μM $FeCl_3$ + 1 mM H_2O_2, but it was not affected by a 1 mT, 50-Hz magnetic field.

4. Discussion

Li and Chow (2001) demonstrated that the degradation of plasmid DNA by Cu^{2+} + H_2O_2 is accelerated by a 50-Hz magnetic field. The present study reached the same conclusion, but extended their study by quantifying the degree of the conversion in the presence of lower concentrations of Cu^{2+} ions. The time course shown in the main graph of Figure 5 suggests that the degradation of plasmid DNA by 1 μM Cu^{2+} + 1 mM H_2O_2 occurred through a single DSB at an early stage, which was followed by multiple DSBs. The degradation of DNA fragments was accelerated at later stages by exposure to a magnetic field. This result is presented in the inset of Figure 5 and confirms the previous result (Li and Chow, 2001).

Sagripanti and Kraemer (1989) demonstrated that the reaction between Cu^{2+} + H_2O_2 also causes strand breaks in plasmid DNA and involves radicals, including OH radical. They reported that in the presence of 1 μM Cu^{2+} + 0.1 mM H_2O_2, the amount of supercoiled plasmid pZ189 (5504bp) decreased to ~70% after 90 min incubation at 37 °C. In our case, the amount of plasmid supercoiled DNA decreased to ~35% after 90 min incubation at room temperature (24 °C) in the presence of 1 μM Cu^{2+} + 1 mM H_2O_2. We presume that a similar or the same chemical process occurred in both the present study and in the Sagripanti and Kraemer study.

Based on their results, Sagripanti and Kraemer (1989) proposed a mechanism for the strand breaks in the presence of $Cu^{2+} + H_2O_2$: a proton translocates from a Cu^{2+} ion to a guanine of DNA to produce a Cu^{+} ion, and a reaction between the Cu^{+} ion and H_2O_2 produces an OH radical, which acts to break the DNA strand. We speculate that a 50-Hz magnetic field may accelerate some of these steps, for example, the rate of the proton translocation: it may depend on the relative orientation of the spin of proton and DNA. The external magnetic field would affect the orientation of the spin thereby changing the rate of the translocation and hence, the formation of Cu^{+} ions.

The absence of an effect of the magnetic field on the degradation of plasmid by the enzymatic reaction of horseradish peroxidase on H_2O_2 can be understood along similar lines to a previous result demonstrating that a magnetic field does not affect the reaction of horseradish peroxidase on H_2O_2 (Jones et al., 2006).

In the present study, the degradation of plasmid by the Fe-Fenton reaction was unaffected by a magnetic field. We presume that both the presence of OH radical and the type of metal ion are important factors in the acceleration effect of a magnetic field, although different experimental conditions, such as different valence of Fe ions (Fe^{3+} instead of Fe^{2+}) and different H_2O_2 concentrations, or different flux densities, may contribute to the effect of the magnetic field.

The flux density of the magnetic field used in our experiments (1.2 mT) is much higher (> 1000 times) than our daily exposure and exceeds the upper limit of occupational exposure (1 mT) set by the International Commission on Non-Ionizing Radiation Protection (ICNIRP, 2010). Furthermore, the concentration of Cu^{2+} ions in the cell has been reported to be much lower than 1 μM (Wataha et al., 1994; Rea et al., 1999). In addition, the intracellular H_2O_2 concentration is well below 1 mM, because significant cellular DNA strand breakage is induced by exogenously added H_2O_2 at extracellular concentrations as low as 0.01 mM (Itsuki Ando, Department of Physics, Tohoku University, unpublished observation). These observations imply that the effect of the magnetic fields on the integrity of DNA is far more enhanced by some condition(s) that is specific to living organisms. To evaluate this notion, future studies under wider experimental conditions (flux density, length of the time for exposure or Cu^{2+}/H_2O_2 concentrations) will be necessary.

5. Conclusion

In the present study we found that 1.2 mT, 50-Hz magnetic field accelerated the degradation of a supercoiled plasmid in the presence of Cu^{2+} ions and H_2O_2. More specifically, the magnetic field accelerated the conversion of the supercoiled plasmid to a linear DNA by a single cleavage of the double-strand. The magnetic field further accelerated the degradation of the linear DNA by multiple double-strand breaks. The mechanism of the acceleration is currently unknown, but the proton translocation form Cu^{2+} ions to DNA guanine, a step that is critical during the strand breaks, may be modulated by the magnetic field.

References

Adair, R. K. (2000). Static and low-frequency magnetic field effects: Health risks and therapies. *Reports on Progress in Physics*, *63*, 415-454. https://doi.org/10.1088/0034-4885/63/3/204

Babbs, C. F., & Gale, M. J. (1988). Colorimetric assay for methane sulfinic acid in biological samples. *Analytical Biochemistry*, *163*, 67-73. https://doi.org/10.1016/0003-2697(87)90093-5

Barreto, J. C., Smith, G. S., Strobel, N. H. P., McQuillin, P. A., & Miller, T. A. (1995). Terephthalic acid: a dosimeter for the detection of hydroxyl radicals in vitro. *Life Sciences*, *56*, PL89-96.

Chen, S. X., & Schopfer, P. (1999). Hydroxyl-radical production in physiological reactions. *European Journal of Biochemistry*, *260*, 726-735. https://doi.org/10.1046/j.1432-1327.1999.00199.x

Focke, F., Schuermann, D., Kuster, N., & Schär, P. (2010). DNA fragmentation in human fibroblasts under extremely low frequency electromagnetic field exposure. *Mutation Research - Fundamental Molecular Mechanisms of Mutagenesis*, *683*, 74-83. https://doi.org/10.1016/j.mrfmmm.2009.10.012

Henle, E. S., & Linn, S. (1997). Formation, prevention, and repair of DNA damage by iron/hydrogen peroxide. *The Journal of Biological Chemistry*, *272*, 19095-19098. https://doi.org/10.1074/jbc.272.31.19095

Hicks, M., & Gebicki, J. M. (1986). Rate constants for reaction of hydroxyl radicals with Tris, Tricine and Hepes buffers. *FEBS Letters*, *199*, 92-94. https://doi.org/10.1016/0014-5793(86)81230-3

International commission on non-ionizing radiation protection (ICNIRP). (2010). Guidelines for limiting exposure to time-varying electric and magnetic fields (1 Hz - 100 kHz). *Health Physics*, *99*, 818-836. https://doi.org/10.1097/HP.0b013e3181f06c86

Jaite, J., Zmyslony, M., Palus, J., Dziubaltowska, E., & Rajkowska, E. (2001). Protective effect of melatonin against in vitro iron ions and 7 mT 50 Hz magnetic field-induced DNA damage in rat lymphocytes. *Mutation Research*, *483*,

57-64. https://doi.org/10.1016/S0027-5107(01)00230-5

Jones, A. R., Scrutton, N. S., & Woodward, J. R. (2006). Magnetic field effects and radical pair mechanisms in enzymes: a reappraisal of the horseradish peroxidase system. *The Journal of American Chemical Society*, *128*, 8408-8409.

Kastir, G., & Parola, H. (1998). Enhanced proliferation caused by a low frequency weak magnetic field in chick embryo fibroblasts is suppressed by radical scavengers. *Biochemical and Biophysical Research Communications*, *252*, 753-756. https://doi.org/10.1006/bbrc.1998.9579

Lai, H., & Singh, N. P. (2004). Magnetic field-induced DNA strand breaks in brain cells of the rat. *Environmental Health Perspectives*, *112*, 687-694. https://doi.org/10.1289/ehp.6355

Li, S. H., & Chow, K. C. (2001). Magnetic field exposure induces DNA degradation. *Biochemical and Biophysical Research Communications*, *286*, 1385-1388. https://doi.org/10.1006/bbrc.2001.4286

Luo, Y., Zhengxu, X. H., Chin, S. M., & Linn, S. (1994). Three chemically distinct types of oxidants formed by iron-mediated Fenton reactions in the presence of DNA. *Proceedings of the National Academy of Sciences* (*USA*), *91*, 12438-12442. https://doi.org/10.1073/pnas.91.26.12438

Mattsson, M. O., & Simkó, M. (2012). Is there a relation between extremely low frequency magnetic field exposure, inflammation and neurodegenerative diseases? A review of in vivo and in vitro experimental evidence. *Toxicology*, *301*, 1-12. https://doi.org/10.1016/j.tox.2012.06.011

Nakayama, M., Hondou, T., & Miyata, H. (2014). DNA strand breaks in fibroblasts exposed to a 50-Hz magnetic field. *JPS Conference Proceedings*, *1*, 012057-1-4. ISBN: 978-4-89027-101-6. https://doi.org/10.7566/JPSCP.1.012057

Nakayama, M., Nakamura, A., Hondou, T., & Miyata, H. (2016). Evaluation of cell viability, DNA single-strand breaks, and nitric oxide production in LPS stimulated macrophage RAW264 exposed to a 50-Hz magnetic field. *International Journal of Radiation Biology*, *92*, 583-589. https://doi.org/10.1080/09553002.2016.1206224

Potenza, L., Cuccharini, L., Piatti, E., Angelini, U., & Dacha, M. (2004). Effects of high static magnetic field exposure on different DNAs. *Bioelectromagnetics*, *25*, 352-355. https://doi.org/10.1002/bem.10206

Rea, T. D., Schmidt, P. J., Pufahl, R. A., Culotta, V. C., & O'Halloran, T. V. (1999) Undetectable Intracellular Free Copper: The Requirement of a Copper Chaperone for Superoxide Dismutase. *Science*, *284*, 805-808. https://doi.org/10.1126/science.284.5415.805

Romanova, T. A., Levites, L. M., & Kuleshova, M. G. (1980). Spectrophotometric analysis of hydrazine sulfate and terephthalic acid in the coagulation bath and wash water of oksalonfibre. [English translation from] *Khimicheskie Volokna*, *1*, 57-58.

Sagripanti, J. L., & Kraemer, K. H. (1989). Site-specific oxidative DNA damage at polyguanosines produced by copper plus hydrogen peroxide. *Journal of Biological Chemistry*, *264*, 1729-1734.

Takeshita, S., Sato, M., Toba, M., Masahashi, W., & Hashimoto-Gotoh, T. (1987). High-copy-number and low-copy-number plasmid vectors for lacZ-complementation and chloramphenicol- or kanamycin-resistance selection. *Gene*, *61*, 63-74. https://doi.org/10.1016/0378-1119(87)90365-9

Wataha, J. C., Hanks, C. T., & Craig R. G. (1994). In vitro effects of metal ions on cellular metabolism and the correlation between these effects and the uptake of the ions. *Journal of Biomedical Materials Research*, *28*, 427-433. https://doi.org/10.1002/jbm.820280404

Yamazaki, I., & Piette, L. H. (1991). EPR spin-trapping study on the oxidizing species formed in the reaction of the ferrous ion with hydrogen peroxide. *Journal of the American Chemical Society*, *113*, 7588-7593. https://doi.org/10.1021/ja060504i

Zmyslony, M., Palus, J., Jaite, J., Dziubaltowska, E., & Rajkowska, E. (2000). DNA damage in rat lymphocytes treated in vitro with iron cations and exposed to 7 mT magnetic fields (static or 50 Hz). *Mutation Research*, *453*, 89-96. https://doi.org/10.1016/S0027-5107(00)00094-4